World Academy of Science, Engineering and Technology
International Journal of Electrical and Computer Engineering
Vol:8, No:2, 2014

Comparison between PI and PR Current Controllers in Grid Connected PV Inverters

D. Zammit, C. Spiteri Staines, M. Apap

***Abstract*—**This paper presents a comparison between Proportional Integral (PI) and Proportional Resonant (PR) current controllers used in Grid Connected Photovoltaic (PV) Inverters. Both simulation and experimental results will be presented. A 3kW Grid-Connected PV Inverter was designed and constructed for this research.

***Keywords*—**Inverters, Proportional-Integral Controller, Proportional-Resonant Controller, Photovoltaic.

Open Science Index, Electrical and Computer Engineering Vol:8, No:2, 2014 publications.waset.org/9997375/pdf

I. Introduction

GRID-CONNECTED PV Inverter systems have become an important power generating method and the number of these systems connected to the grid is always increasing. Therefore it is important to limit the harmonics generated by these inverters to limit adverse effects on the grid power quality. This means that the design of these inverters should follow harmonic limits set by IEEE and European IEC standards (IEEE 929, IEEE 1547 and IEC 61727) which suggest limits for the current total harmonic distortion (THD) factor and also for the magnitude of each harmonic.

The current controller can have a significant effect on the quality of the current supplied to the grid by the PV inverter, and therefore it is important that the controller provides a high quality sinusoidal output with minimal distortion to avoid creating harmonics. Two controllers which are used in current-controlled PV inverters are the PI controller with the grid voltage feed-forward and the PR controller.

Comparison of the two controllers is presented and discussed in [1]-[3] among others. A shortcoming with the PI controller generally is that it is not able to follow a sinusoidal reference without steady state error due to the dynamics of the integral term. The inability to track a sinusoidal reference causes the need to use the grid voltage as a feed-forward term to obtain a good dynamic response by helping the controller to try to reach steady state faster. A current controller which is more suited to operate with sinusoidal references and does not suffer from the above mentioned drawback is the PR controller. The PR controller provides gain at a certain frequency (resonant frequency) and almost no gain exists at the other frequencies.

In this paper the design of a single phase 3kW grid-connected PV inverter is presented, which includes the design of the LCL filter and the current control. A comparison between PI and PR current controllers used in grid-connected PV inverters is also presented, both by simulations and by experimental tests.

Fig. 1 below shows a block diagram of the Grid-Connected PV Inverter system connected to the grid through an LCL filter.

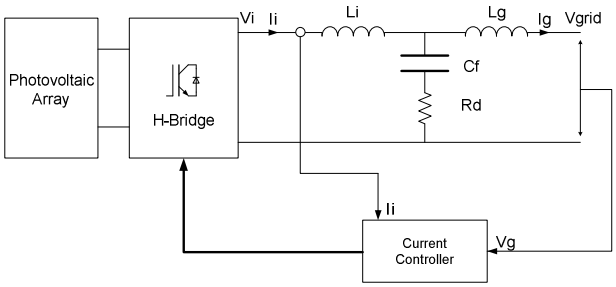


Fig. 1 Block diagram of the Grid-Connected PV Inverter with the LCL Filter

II. LCL Filter and Current Control

A. LCL Filter

The transfer function of the LCL filter in terms of the inverter current I_i and the inverter voltage U_i, neglecting R_d, is:

$$G_F(s) = \frac{I_i}{U_i} = \frac{1}{L_i s} \frac{(s^2 + [1/L_g C_f])}{(s^2 + [(L_i + L_g)/(L_i L_g C_f)])} \quad (1)$$

where, L_i is the inverter side inductor
L_g is the grid side inductor
and C_f is the filter capacitor

The resonant frequency of the filter is given by:

$$\omega_{res} = \sqrt{\frac{(L_i + L_g)}{(L_i L_g C_f)}} \quad (2)$$

The transfer function in (1) does not include the damping resistor R_d. The introduction of R_d in series with the capacitor C_f increases stability and reduces resonance [4]. This method of damping is a type of Passive Damping. Whilst there exist other methods of passive damping and also more advanced Active Damping methods, this particular damping method used was considered enough for the aim and purpose of comparing the two current controllers due to its simplicity. The transfer function of the filter taking in consideration the damping resistor R_d is:

Daniel Zammit, Prof. Cyril Spiteri Staines, and Dr Maurice Apap are with the Department of Industrial Electrical Power Conversion, University of Malta, Msida, MSD 2080 (e-mail: daniel.zammit@um.edu.mt, cyril.spiteri-staines@um.edu.mt, maurice.apap@um.edu.mt).

$$G_F(s) = \frac{I_i}{U_i} = \frac{1}{L_i s} \frac{(s^2 + s(R_d/L_g) + [1/L_g C_f])}{(s^2 + s([(L_i + L_g)R_d]/L_i L_g) + [(L_i + L_g)/(L_i L_g C_f)])} \quad (3)$$

B. PI Control with Grid Voltage Feed-Forward

Fig. 2 below shows the PI current control strategy with the grid voltage feed-forward (U_G). I_i is the inverter output current which is used as feedback, I_i^* is the inverter current reference and U_i^* is the inverter voltage reference.

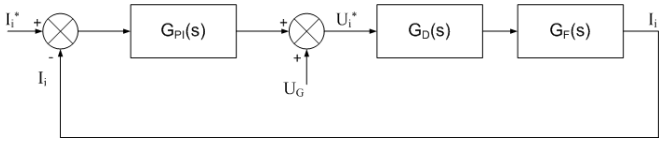


Fig. 2 The PI Current Control with the Grid Voltage Feed-Forward

The PI current controller $G_{PI}(s)$ is represented by:

$$G_{PI}(s) = K_P + \frac{K_I}{s} \quad (4)$$

where, K_P is the Proportional Gain term and K_I is the Integral term.

$G_F(s)$ represents the LCL filter. $G_D(s)$ represents the processing delay of the microcontroller, which is typically equal to the time of one sample T_s and is represented by:

$$G_D(s) = \frac{1}{1 + sT_s} \quad (5)$$

C. PR Control

Fig. 3 below shows the PR current control strategy. I_i is the inverter output current which is used as feedback, I_i^* is the inverter current reference and U_i^* is the inverter voltage reference.

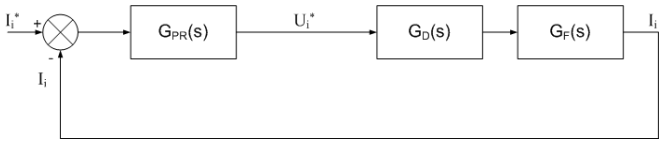


Fig. 3 The PR Current Control

The PR current controller $G_{PR}(s)$ is represented by:

$$G_{PR}(s) = K_P + K_I \frac{s}{s^2 + \omega_0^2} \quad (6)$$

where, K_P is the Proportional Gain term, K_I is the Integral Gain term and ω_0 is the resonant frequency.

The ideal resonant term on its own in the PR controller provides an infinite gain at the ac frequency ω_0 and no phase shift and gain at the other frequencies [5]. The K_P term determines the dynamics of the system; bandwidth, phase and gain margins [5].

Equation (6) represents an ideal PR controller which can give stability problems because of the infinite gain. To avoid these problems, the PR controller can be made non-ideal by introducing damping as shown in (7) below.

$$G_{PR}(s) = K_P + K_I \frac{2\omega_c s}{s^2 + 2\omega_c s + \omega_0^2} \quad (7)$$

where, ω_c is the bandwidth around the ac frequency of ω_0.

With (7) the gain of the PR controller at the ac frequency ω_0 is now finite but it is still large enough to provide only a very small steady state error. This equation also makes the controller more easily realizable in digital systems due to their finite precision [6].

III. LCL Filter Design

To perform comparison tests between the two current control strategies, a 3kW Grid-Connected Inverter was designed and constructed. The LCL filter was designed following the procedure in [5], [7]. Designing for a dc-link voltage of 358V, maximum ripple current of 20% of the grid peak current, a switching frequency of 10kHz, filter cut-off frequency of 2kHz and the reactive power produced by the capacitor not to exceed 5% of rated power, the following values of the LCL filter were obtained: L_i = 1.2mH, L_g = 0.7mH, C_f = 9μF and R_d = 8Ω.

IV. PI and PR Controller Design

A. PI Controller Design

The PI controller was designed for a damping factor in the range of 0.8 and a natural frequency in the range of 3142 rad/sec, obtaining a K_p of 4.21 and K_I of 2107. The damping factor ζ obtained was 0.85 and the natural frequency ω_n obtained was 3360 rad/sec.

Fig. 4 shows the root locus plot in Matlab of the system including the LCL filter, the processing delay, anti-aliasing filter in the output current feedback path and the PI controller. The root locus plot shows that the designed system is stable.

Open Science Index, Electrical and Computer Engineering Vol:8, No:2, 2014 publications.waset.org/9997375/pdf

Open Science Index, Electrical and Computer Engineering Vol:8, No:2, 2014 publications.waset.org/9997375/pdf

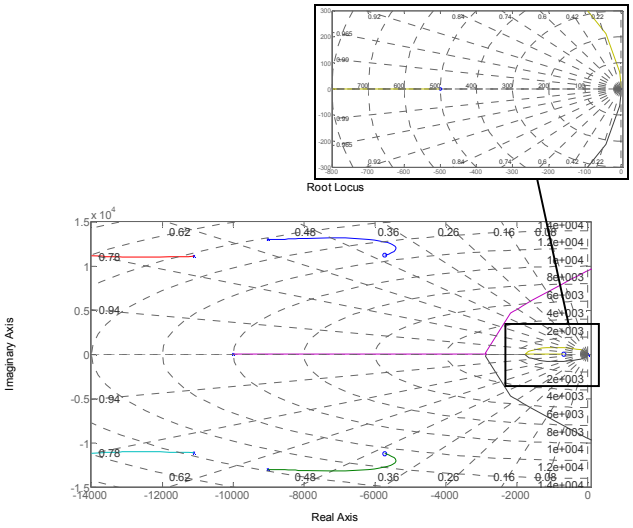


Fig. 4 Root Locus of the Inverter with the PI Controller

Fig. 5 below shows the open loop bode diagram of the system and Fig. 6 shows the closed loop bode diagram of the system. From the open loop bode diagram, the Gain Margin obtained is 17.5dB at a frequency of 9660rad/s and the Phase Margin obtained is 53.6deg at a frequency of 2180rad/s.

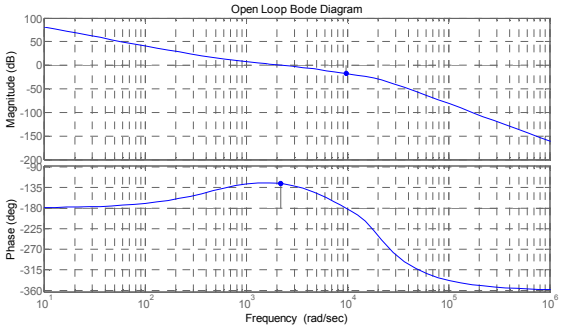


Fig. 5 Open Loop Bode Diagram of the System with PI Control

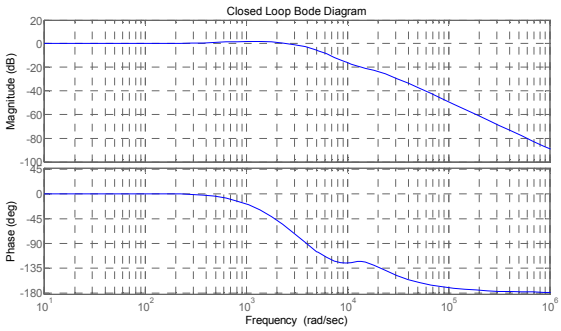


Fig. 6 Closed Loop Bode Diagram of the System with PI Control

B. PR Controller Design

The PR controller was designed for a resonant frequency ω_0 of 314.2rad/s (50Hz) and ω_c was set to be 0.5rad/s, obtaining a K_p of 5.1 and K_I of 2073.15.

Fig. 7 below shows the root locus plot in Matlab of the system including the LCL filter, the processing delay, anti-aliasing filter in the output current feedback path and the PR controller. The root locus plot shows that the designed system is stable.

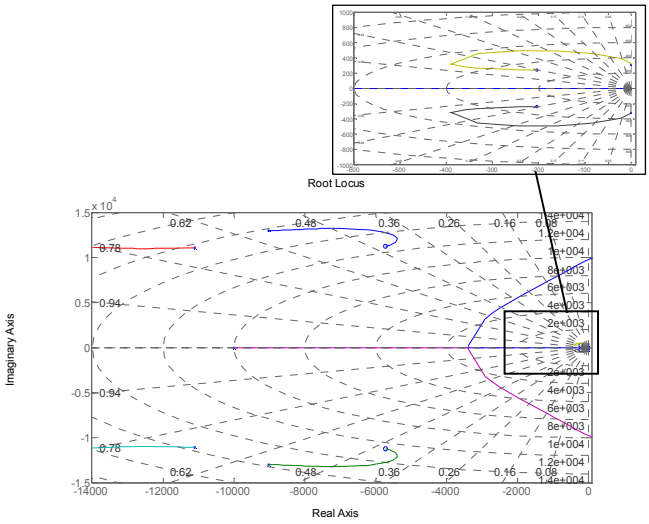


Fig. 7 Root Locus of the Inverter with the PR Controller

Fig. 8 below shows the open loop bode diagram of the system and Fig. 9 shows the closed loop bode diagram of the system. From the open loop bode diagram, the Gain Margin obtained is 16.1dB at a frequency of 9760rad/s and the Phase Margin obtained is 53.2deg at a frequency of 2570rad/s.

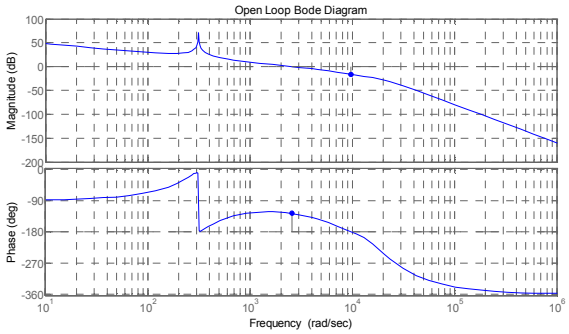


Fig. 8 Open Loop Bode Diagram of the System with PR Control

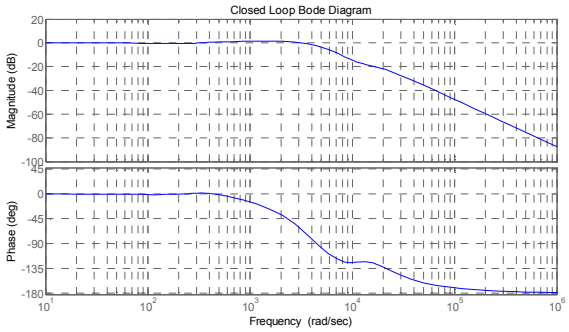


Fig. 9 Closed Loop Bode Diagram of the System with PR Control

Open Science Index, Electrical and Computer Engineering Vol:8, No:2, 2014 publications.waset.org/9997375/pdf

V. SIMULATIONS

The 3kW Grid-Connected PV Inverter was modeled and simulated in Simulink with PLECS blocksets, both in the s-domain and the z-domain.

Figs. 10 and 11 below show the grid voltage (V_{grid}), the inverter current (I_{inv}), the grid current (I_{grid}) and the reference current (I_{ref}) from the simulation using the PI controller and from the simulation using the PR controller, respectively.

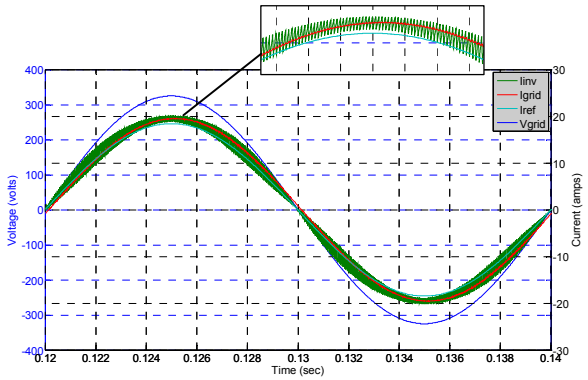


Fig. 10 Grid Voltage, Inverter Current, Grid Current and Reference Current from Simulation using the PI Controller

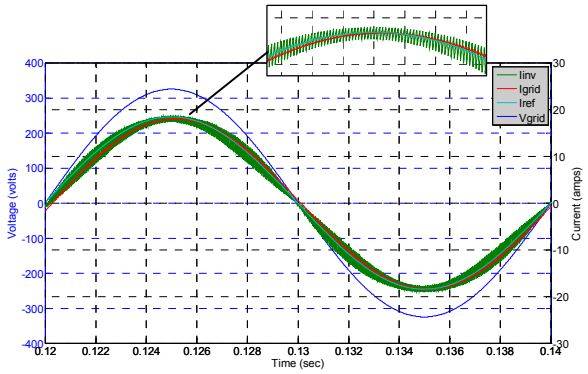


Fig. 11 Grid Voltage, Inverter Current, Grid Current and Reference Current from Simulation using the PR Controller

From the simulation results shown in Fig. 10 the PI current controller has a considerable steady state error when following the reference current, resulting in a difference of approximately 3% between the reference current and the inverter current. The steady state error is less for the PR current controller, practically negligible, as can be seen in the simulation results in Fig. 11. The small steady state error in the inverter current when using the PR controller is due to the use of a non-ideal PR controller, as this avoids controller stability problems.

VI. GRID-CONNECTED PV INVERTER TESTING

The constructed 3kW Grid-Connected PV Inverter test rig is shown in Fig. 12 below. It was operated at a switching frequency of 10kHz and was connected to a 50Hz grid supply. The inverter was controlled by the dsPIC30F4011 microcontroller from Microchip. The inverter was tested using the PI and the PR controllers to compare the performance of the two current controllers. The inverter was connected to the grid using a variac to allow variation of the grid voltage for testing purposes. The dc link voltage was obtained using a dc power supply.

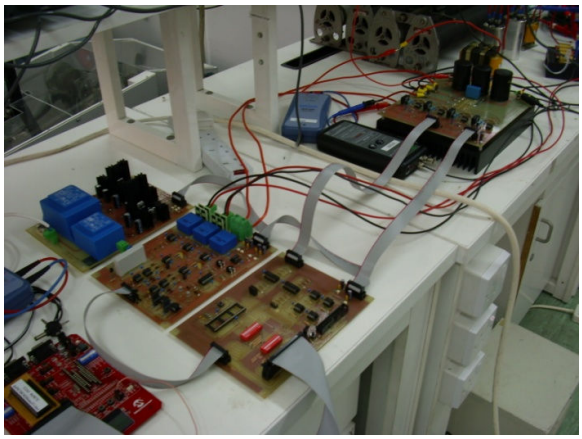


Fig. 12 3kW Grid-Connected PV Inverter Test Rig

Figs. 13 and 14 below show the inverter output voltage, the grid voltage and the grid current for a dc-link voltage of 300V, a grid voltage of 150V and a preset value of 8A peak using the PI controller and the PR controller, respectively.

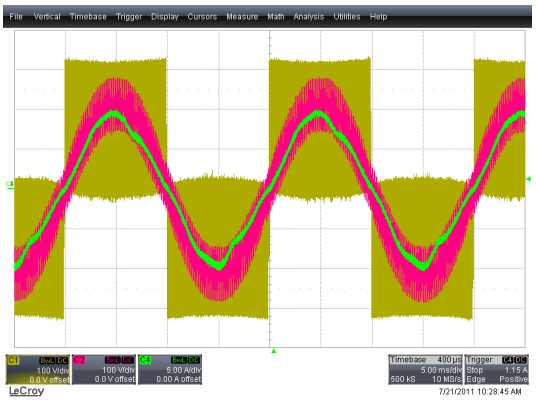


Fig. 13 Inverter Output Voltage, Grid Voltage and Grid Current with a Preset Current of 8A Peak using the PI Controller

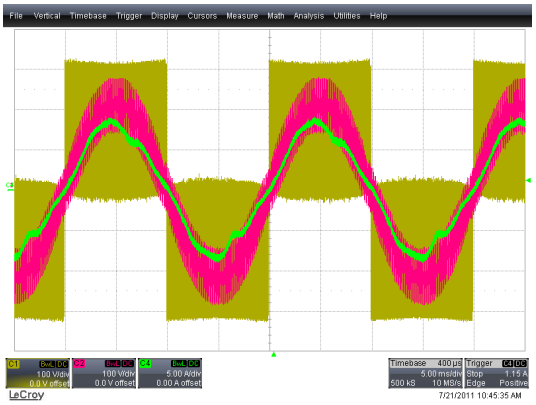


Fig. 14 Inverter Output Voltage, Grid Voltage and Grid Current with a Preset Current of 8A Peak using the PR Controller

Open Science Index, Electrical and Computer Engineering Vol:8, No:2, 2014 publications.waset.org/9997375/pdf

Figs. 15 and 16 show the grid current for the grid-connected inverter with the PI current controller and with the PR current controller, respectively. I_g is the grid current, I_{gr} is the reconstructed grid current up to its 13th harmonic (a reconstruction of the grid current by adding the first 13 lower harmonics) and I_{gfund} is the fundamental component of the grid current.

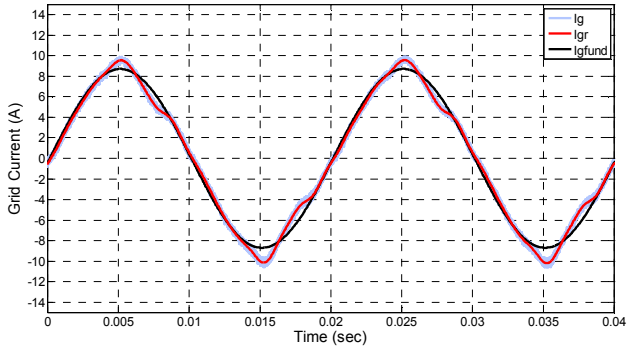


Fig. 15 Grid Current with PI Current Control

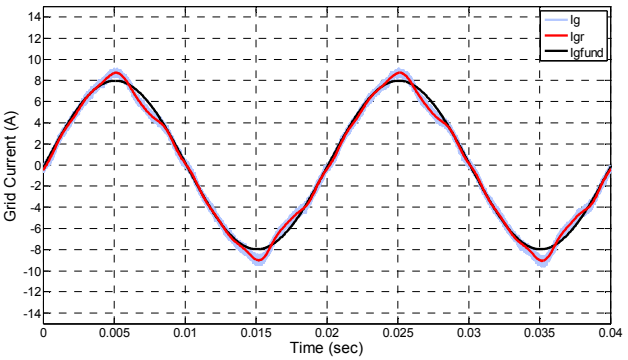


Fig. 16 Grid Current with PR Current Control

Figs. 17 and 18 show the harmonic spectrum of the grid current with the PI current controller and with the PR current controller, respectively. When the PI current controller was used the fundamental component of the grid current reached about 108.815% of the expected 8A peak, due to the steady state error drawback of the controller. The 3rd, 5th and 7th harmonics resulted about 8.252%, 4.771% and 2.728%, respectively. When the PR current controller was used the fundamental component of the grid current reached 100% of the expected 8A peak. The 3rd, 5th and 7th harmonics reached about 5.574%, 4.231% and 2.435%, respectively.

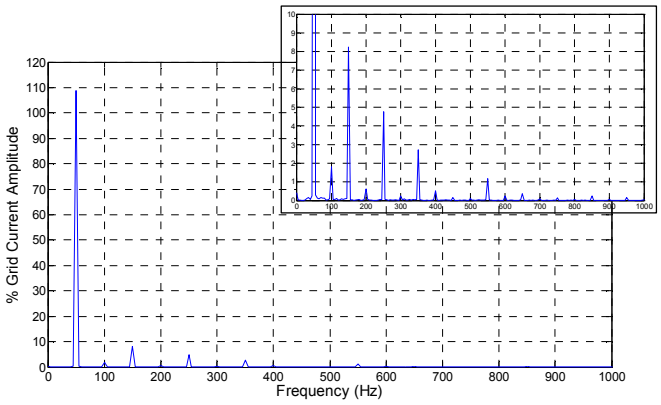


Fig. 17 Harmonic Spectrum of the Grid Current with PI Current Control

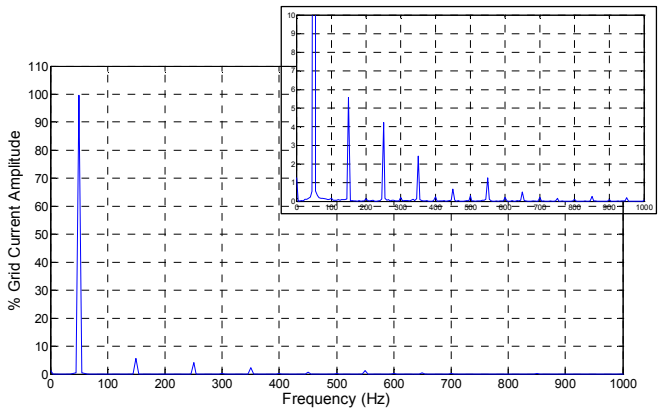


Fig. 18 Harmonic Spectrum of the Grid Current with PR Current Control

VII. Comparison of Experimental Results

In the actual results obtained from the grid-connected inverter there is a larger steady state error when using the PI current controller than when using the PR current controller, as was expected. This agrees with the results obtained in the simulations.

When the inverter is controlled by the PI controller, with a 50Hz sinusoidal reference current of 8A peak, the resulting fundamental inverter current peak is approximately 8.72A, as shown in Fig. 15. This results in a percentage error of approximately 9%. The difference in the percentage error between the simulation result and the practical result is due to non-idealness in the practical inverter when compared to the ideal inverter modeled in the simulation.

When the inverter is controlled by the PR controller, for the same sinusoidal reference current of 8A peak, the resulting fundamental inverter current peak is 8A, as shown in Fig. 14. This yields a 0% percentage error. Although a small error was expected due to the fact that the non-ideal (damped) version of the PR controller was used, it did not result in this case since the value of ω_c was kept very small at 0.5rad/s. And, thus the resonant term gain, although reduced, it was still large enough to follow the reference without problems. With the PR controller there was no need for the grid voltage feed-forward

term to track the current reference.

When considering the 3rd, 5th and 7th harmonics resulted in the grid current with the two types of current controllers, although in this case the harmonics are less when using the PR current controller, in both cases are higher than the limits allowed by the standard regulations. The IEEE 929 and IEEE 1547 standards allow a limit of 4% for each harmonic from 3rd to 9th and 2% for 11th to 15th [8], [9]. The IEC 61727 standard specifies similar limits [10]. As can be observed from the results, the 3rd and 5th harmonics with both current controllers are outside the limits. These harmonics result from the inverter itself due to the non-linearities in the inverter and also from the grid supply.

These results demonstrate that although the PR controller is superior to the PI controller when following a sinusoidal reference, additional harmonic compensation is needed in both cases to be compliant with the limits allowed by the standard regulations.

VIII. Conclusion

This paper has presented a comparison between standard PI and PR current controllers in Grid-Connected PV Inverters. Results from simulations and experimental analysis of a 3kW inverter connected to the 50Hz grid are shown. Both simulation and experimental results show that a PI controller with voltage feed-forward suffered from a steady state error when following a sinusoidal reference. In the experimental results obtained when using the PI controller there was an error of approximately 9% in the grid current fundamental in following the current reference. This error is reduced to zero when using the PR controller. Regarding the 3rd, 5th and 7th harmonics in the grid current, from the results obtained with both controllers the 3rd and 5th harmonics were outside the permissible limits. Thus although these results demonstrate the superiority of the PR controller for applications requiring sinusoidal references, additional harmonic compensation is needed in both cases to conform to the standard regulations.

References

[1] R. Teodorescu, F. Blaabjerg, U. Borup, M. Liserre, "A New Control Structure for Grid-Connected LCL PV Inverters with Zero Steady-State Error and Selective Harmonic Compensation", APEC'04 Nineteenth Annual IEEE Conference, California, 2004.

[2] M. Liserre, R. Teodorescu, Z. Chen, "Grid Converters and their Control in Distributed Power Generation Systems", IECON 2005 Tutorial, 2005.

[3] M. Ciobotaru, R. Teodorescu, F. Blaabjerg, "Control of a Single-Phase PV Inverter", EPE2005, Dresden, 2005.

[4] V. Pradeep, A. Kolwalkar, R. Teichmann, "Optimized Filter Design for IEEE 519 Compliant Grid Connected Inverters", IICPE 2004, Mumbai, India, 2004.

[5] R. Teodorescu, M. Liserre, P. Rodriguez, "Grid Converters for Photovoltaic and Wind Power Systems", Wiley, 2011.

[6] D. N. Zmood, D. G. Holmes, "Stationary Frame Current Regulation of PWM Inverters with Zero Steady-State Error", IEEE Transactions on Power Electronics, Vol. 18, No. 3, May 2003.

[7] M. Liserre, F. Blaabjerg, S. Hansen, "Design and Control of an LCL-Filter Based Three Phase Active Rectifier", IEEE Transactions on Industry Applications, Vol 41, No. 5, Sept/Oct 2005.

[8] IEEE 929 2000 Recommended Practice for Utility Interface of Photovoltaic (PV) Systems.

[9] IEEE 1547 Standard for Interconnecting Distributed Resources with Electric Power Systems.

[10] IEC 61727 2004 Standard Photovoltaic (PV) Systems – Characteristics of the Utility Interface.

Open Science Index, Electrical and Computer Engineering Vol:8, No:2, 2014 publications.waset.org/9997375/pdf